A New Method for Eye Location Tracking

Eugene Paperno* and Dmitry Semyonov

***Abstract*—A standard scleral search coil (SSC) system is supplied with a single three-axial transmitter (or with a triad of transmitters) and the *direct* magnetic coupling between the transmitting coils and the SSC is used for computing the eye location. The SSC's orientation components measured by the SSC system are involved in the location-tracking algorithm as well. The suggested method differs from traditional ones where the eye location is computed *indirectly*, relative to the measured location and orientation of a *transitional* three-axial magnetic sensor attached to the subject's head. The new method eliminates systematic errors caused by inaccurate situating the transitional sensor relative to the eye. It also eliminates systematic errors caused by imperfect orthogonality of the transitional sensor.**

It is found that an accurate location tracking with a single transmitter is possible only if orientation freedom of the eye is limited. To track the eye location with no orientation limitations, a triad of transmitters is employed. The resulting accuracy can be as good as ± 1 mm (in a 200-Hz bandwidth) over a relatively large ($0.5 \times 0.5 \times 0.5$ m) operating region in the center of a $1 \times 1 \times 1$ m SSC system. The analytical results obtained are confirmed with the help of computer simulations.

***Index Terms*—Direct magnetic coupling, eye location tracking, scleral search coil, triad of there-axial transmitters.**

I. Introduction

THE magnetic scleral search coil (SSC) technique [1]–[4] is a standard research tool used for monitoring eye movements in man and experimental animals. A typical SSC system (see Fig. 1) consists of a field coil box and an SSC embedded in modified contact lens. The field coil box is combined from two or three pairs of induction coils mounted to the sides of a cube. The size of a typical field coil box ranges from 0.3 to 2 m.

The SSC technique is based on amplitude detection of the voltages induced in the SSC by the field coils. The amplitudes of the induced voltages are linear functions of the SSC's axis unit vector components, $\vec{s} = (s_1, s_2, s_3)$, and trigonometric functions of the azimuth and elevation angles, θ and ψ (see Fig. 1).

The advantage of the SSC technique is that it provides a high temporal (up to 4 kHz) and angular (up to 0.005° [4]) resolution. This allows for effortless recording even the smallest types of angular eye movements.

In many applications there is a need to measure not only the eye orientation, but the eye location as well. It is traditionally done by an *indirect* method. The SSC system is supplied with a conventional magnetic tracker [5] consisting of a three-axial transmitter located outside the field coil box and a *transitional* three-axial magnetic sensor attached to the subject's head (see Fig. 1). The eye location is calculated relative to the measured location and orientation of the transitional sensor.

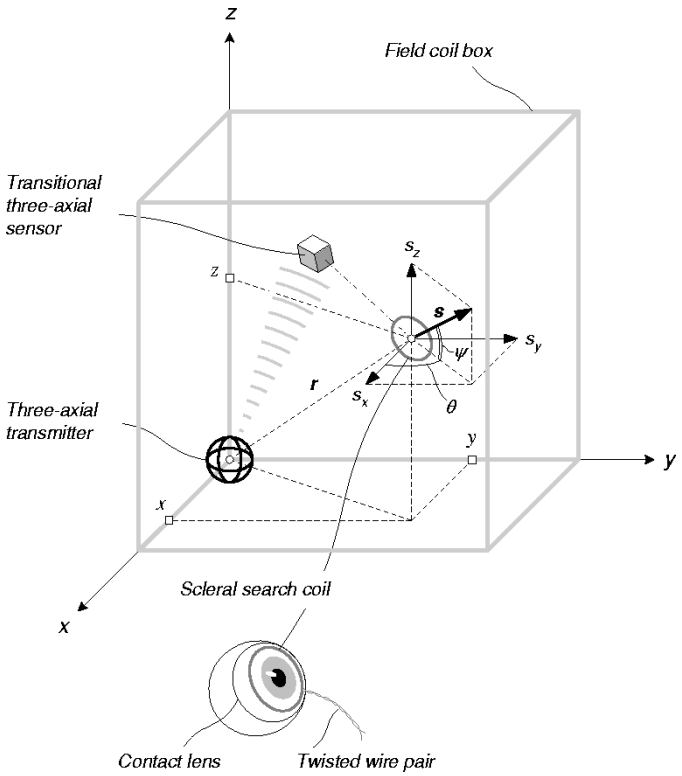

Fig. 1. A typical SSC system. To track the eye location, a conventional magnetic tracker consisting of the three-axial transmitter and the *transitional* three-axial magnetic sensor is added to the system. The three-axial transmitter is located outside the field coil box, and the transitional sensor is attached to the subject's head. The eye location, $\vec{r} = (x, y, z)$, is calculated *indirectly*, relative to the measured location and orientation of the transitional magnetic sensor.

It is important, however, to track the eye location by a *direct* method. This should eliminate systematic errors caused by inaccurate situating the transitional sensor relative to the eye. It should also eliminate systematic errors caused by imperfect orthogonality of the transitional sensor.

For tracking the eye location *directly*, with no transitional sensor, we investigate the possibility of employing the direct magnetic coupling between the three-axial transmitter—or a number of transmitters—and the SSC itself.

Our aim is to provide theoretical groundings for upcoming experimental work.

II. Eye Location Tracking With a Single Three-Axial Transmitter

To take advantage of the direct magnetic coupling between the three-axial transmitter and the SSC, we suggest involving

Manuscript received August 28, 2002; revised March 18, 2003. This work was supported in part by the Ivanier Center for Robotics Research Ivanier Center for Robotics Research and Production Management. *Asterisk indicates corresponding author.*

*E. Paperno is with the Department of Electrical and Computer Engineering, Ben-Gurion University of the Negev, P.O. Box 653, Beer-Sheva 84105, Israel (e-mail: paperno@ee.bgu.ac.il).

D. Semyonov is with the Department of Electrical and Computer Engineering, Ben-Gurion University of the Negev, Beer-Sheva 84105, Israel.

Digital Object Identifier 10.1109/TBME.2003.817635

in the location-tracking algorithm the orientation components, $\vec{s} = (s_1, s_2, s_3)$, taken from the SSC system's output.

To find the SSC's location $\vec{r} = (x, y, z)$ in Fig. 1, we shall write equations for the quasistatic coupling between the individual transmitting coils and the SSC. Let us assume that number 1 (x directed), number 2 (y directed), and number 3 (z directed) transmitting coils are operated at different frequencies (time and phase sharing can also be used in practice). Corresponding field amplitudes, H_{si}, seen by the SSC can be found in this case as the dot products of the vector $\vec{s}$ and the dipole field vectors, $\vec{H}_i$, generated at the location $\vec{r}$ by the corresponding transmitting coils [6]

$$H_{si} = \vec{H}_i \cdot \vec{s} = \frac{1}{4\pi}\left[\frac{3(\vec{m}_i \cdot \vec{r})\vec{r}}{r^5} - \frac{\vec{m}_i}{r^3}\right] \cdot \vec{s} \tag{1}$$

where $r = |\vec{r}|$ is the magnitude of the vector $\vec{r}$, $\vec{m}_i$ are the magnetic moments of the corresponding transmitting coils, index i runs from 1 to 3 and represents magnetic moments of different transmitting coils, $m_i = |\vec{m}_i| = NAI$, N is the number of turns, A is the area, and I is amplitude of the ac current flowing through the each transmitting coils.

For $m_1 = m$, (1) can be rewritten as follows:

$$\begin{cases} H_{s1} = \frac{m}{4\pi}\frac{3x(\vec{r}\cdot\vec{s}) - s_1 r^2}{r^5} \\ H_{s2} = \frac{m}{4\pi}\frac{3y(\vec{r}\cdot\vec{s}) - s_2 r^2}{r^5} \\ H_{s3} = \frac{m}{4\pi}\frac{3z(\vec{r}\cdot\vec{s}) - s_3 r^2}{r^5} \end{cases} \tag{2}$$

where $s_j = |\vec{s}_j|$, index j runs from 1 to 3 and represents different components of the vector $\vec{s}$, and the dot product $(\vec{r}\cdot\vec{s}) = xs_1 + ys_2 + zs_3$.

The system of (2) can be solved first for

$$r = \sqrt[3]{\frac{m}{4\pi}\frac{1}{2H_s^2}\left[(\vec{H}_s \cdot \vec{s}) + \sqrt{8H_s^2 + (\vec{H}_s \cdot \vec{s})^2}\right]} \tag{3}$$

and then for the SSC's coordinates

$$\begin{cases} x = \frac{\frac{4\pi}{m}r^3 H_{s1} + s_1}{\sqrt{3r}\sqrt{\frac{1}{r^3} + \frac{4\pi}{m}(\vec{H}_s\cdot\vec{s})}} \\ y = \frac{\frac{4\pi}{m}r^3 H_{s2} + s_2}{\sqrt{3r}\sqrt{\frac{1}{r^3} + \frac{4\pi}{m}(\vec{H}_s\cdot\vec{s})}} \\ z = \frac{\frac{4\pi}{m}r^3 H_{s3} + s_3}{\sqrt{3r}\sqrt{\frac{1}{r^3} + \frac{4\pi}{m}(\vec{H}_s\cdot\vec{s})}} \end{cases} \tag{4}$$

where H_{s1}, H_{s2}, and, H_{s3} are the components of a dummy vector $\vec{H}_s = (H_{s1}, H_{s2}, H_{s3})$, such that $H_s^2 = H_{s1}^2 + H_{s2}^2 + H_{s2}^2$ and the dot product $(\vec{H}_s \cdot \vec{s}) = H_{s1}s_1 + H_{s2}s_2 + H_{s3}s_3$.

Once the SSC's coordinates have been found, it is important to estimate the location resolution (rms error) of the method

$$\sigma_{|\Delta\vec{r}|} = \sqrt{\sigma_x^2 + \sigma_y^2 + \sigma_z^2} \tag{5}$$

were σ_x, σ_y, and σ_z are the rms errors of the coordinate estimates.

To find the σ_x, σ_y, and σ_z errors, we suppose that uncorrelated white-noise signals ξ_{s_j} and $\xi_{H_{si}}$ are superimposed on the corresponding components of the $\vec{s}$ and $\vec{H}_s$ vectors. We also assume that the ξ_{s_j} and $\xi_{H_{si}}$ noise signals are relatively small and their rms values are equal, $\sigma_{s_j} = \sigma_s$ and $\sigma_{H_{si}} = \sigma_{H_s}$.

To estimate the resultant noise we use the following partial derivatives. For example, for the SSC's x coordinate:

$$\xi_x = \sum_{i=1}^{3}\frac{\partial x}{\partial H_{si}}\xi_{H_{si}} + \sum_{j=1}^{3}\frac{\partial x}{\partial s_j}\xi_{s_j} + \frac{\partial x}{\partial r}\xi_r \tag{6}$$

where

$$\xi_r = \sum_{i=1}^{3}\frac{\partial r}{\partial H_{si}}\xi_{H_{si}} + \sum_{j=1}^{3}\frac{\partial r}{\partial s_j}\xi_{s_j}. \tag{7}$$

The substitution of (7) into (6) yields

$$\xi_x = \sum_{i=1}^{3}\left(\frac{\partial x}{\partial H_{si}} + \frac{\partial r}{\partial H_{si}}\frac{\partial x}{\partial r}\right)\xi_{H_{si}} + \sum_{j=1}^{3}\left(\frac{\partial x}{\partial s_j} + \frac{\partial r}{\partial s_j}\frac{\partial x}{\partial r}\right)\xi_{s_j}. \tag{8}$$

We assume that the SSC is not moving during each measuring cycle. As a result, the partial derivatives in (8) become constants and can be considered as independent. Thus, we can find the $\sigma_{|\Delta\vec{r}|}$ components by applying Gauss's error propagation rule

$$\begin{cases} \sigma_x = \sqrt{\sigma_{H_s}^2\sum_{i=1}^{3}\left(\frac{\partial x}{\partial H_{si}} + \frac{\partial r}{\partial H_{si}}\frac{\partial x}{\partial r}\right)^2 + \sigma_s^2\sum_{j=1}^{3}\left(\frac{\partial x}{\partial s_j} + \frac{\partial r}{\partial s_j}\frac{\partial x}{\partial r}\right)^2} \\ \sigma_y = \sqrt{\sigma_{H_s}^2\sum_{i=1}^{3}\left(\frac{\partial y}{\partial H_{si}} + \frac{\partial r}{\partial H_{si}}\frac{\partial y}{\partial r}\right)^2 + \sigma_s^2\sum_{j=1}^{3}\left(\frac{\partial y}{\partial s_j} + \frac{\partial r}{\partial s_j}\frac{\partial y}{\partial r}\right)^2}. \\ \sigma_z = \sqrt{\sigma_{H_s}^2\sum_{i=1}^{3}\left(\frac{\partial z}{\partial H_{si}} + \frac{\partial r}{\partial H_{si}}\frac{\partial z}{\partial r}\right)^2 + \sigma_s^2\sum_{j=1}^{3}\left(\frac{\partial z}{\partial s_j} + \frac{\partial r}{\partial s_j}\frac{\partial z}{\partial r}\right)^2} \end{cases} \tag{9}$$

By taking the partial derivatives in (9) and considering (2), we obtain the $\sigma_{|\Delta\vec{r}|}$ as a function of the SSC's true location $\vec{r}$ and orientation $\vec{s}$, see (10) at the bottom of the page. In a similar way

$$\begin{aligned} \sigma_r &= \sqrt{\sigma_{H_s}^2\sum_{i=1}^{3}\left(\frac{\partial r}{\partial H_{si}}\right)^2 + \sigma_s^2\sum_{j=1}^{3}\left(\frac{\partial r}{\partial s_j}\right)^2} \\ &= \frac{1}{9}\frac{r^2}{(\vec{r}\cdot\vec{s})^2 + r^2} \\ &\quad \times \sqrt{\left(\frac{4\pi}{m}\right)^2 9r^8\sigma_{H_s}^2 + [3(\vec{r}\cdot\vec{s})^2 + r^2]\sigma_s^2}. \end{aligned} \tag{11}$$

To evaluate the $\sigma_{|\Delta\vec{r}|}$ quantitatively, we consider a practical case (see Table I) where $\sigma_{H_s} = 10^{-4}$ (-80 dB) relative to the maximum field intensity measured at a 1-m

$$\begin{aligned} &\sigma_{|\Delta\vec{r}|} \\ &= \frac{1}{9(\vec{r}\cdot\vec{s})^2[(\vec{r}\cdot\vec{s})^2 + r^2]} \\ &\times \sqrt{\left(\frac{4\pi}{m}\right)^2 9^2 r^6(\vec{r}\cdot\vec{s})^2\{(\vec{r}\cdot\vec{s})^2[2(\vec{r}\cdot\vec{s})^2 + r^2 - r^4] + r^4\}\sigma_{H_s}^2 + \{(\vec{r}\cdot\vec{s})^2[2(\vec{r}\cdot\vec{s})^2(9(\vec{r}\cdot\vec{s})^2 + 22r^2) + 25r^4] + r^6\}\sigma_s^2}. \end{aligned} \tag{10}$$

TABLE I
SIGNAL-TO-NOISE RATIO CALCULATION

Transmitting coils*		
average diameter	10	cm
number of turns	400	
wire diameter	0.7	mm
resistance	5.8	Ω
excitation current	1	A 0-to-p
magnetic moment	3.1	A m^2
excitation frequency	50	kHz
Scleral search coil (SSC)		
average diameter	15	mm
number of turns	10	
wire diameter	50	μm
Bandwidth	200	Hz
SSC thermal noise	1.8	nV rms
Preamplifier noise	34	nV rms
Atmospheric noise measured in a 1 Hz bandwidth	0.05	μA/m
Total noise measured at the amplifier input	34.4	nV rms
Maximum signal detected at a 1-m distance	0.35	mV 0-to-p
Signal-to-noise ratio, $H_{s\max}/\sigma_{H_s}$,	80	dB

*The transmitter noise is neglected because its amplitude component is small relative to the signal level, and its phase component can be effectively eliminated due to synchronous detection of the SSC output.

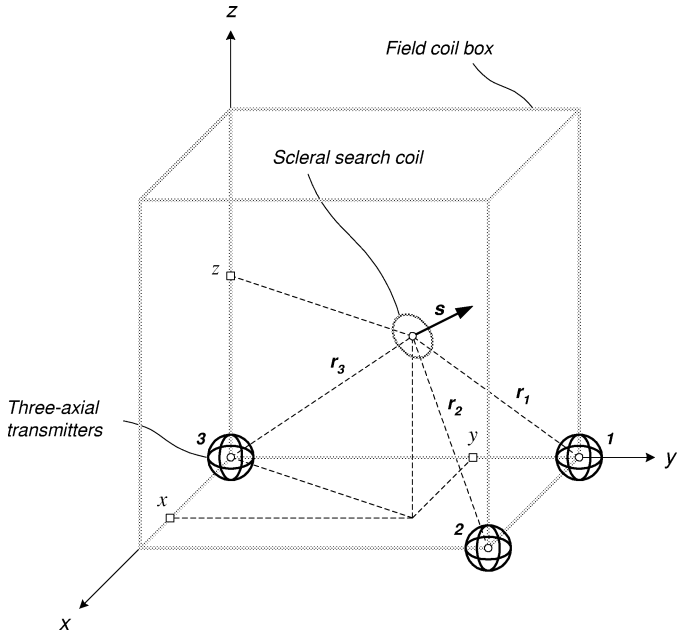

Fig. 3. Eye location tracking with a triad of three-axial transmitters. Finding the distances r_1, r_2, r_3 between the three-axial transmitters and the SSC allows calculation of the eye location by applying the triangulation technique.

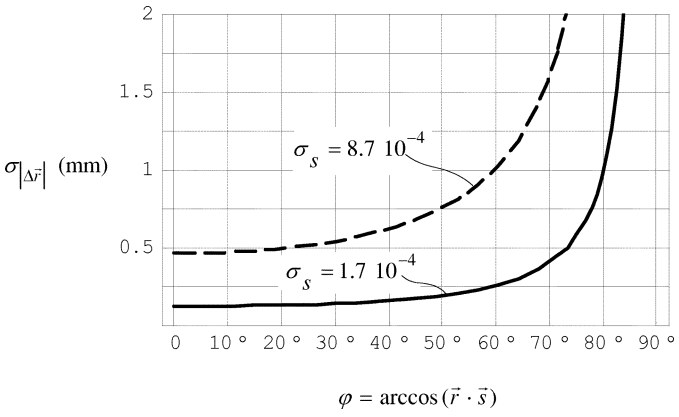

Fig. 2. The location resolution $\sigma_{|\Delta\vec{r}|}$ as a function of the angle φ between the $\vec{r}$ and $\vec{s}$ vectors. The SSC is located at a 1-m distance from the transmitter, such that $\vec{r} = (\sqrt{1/3}, \sqrt{1/3}, \sqrt{1/3})$.

distance from the three-axial transmitter. Then for a fixed $\vec{r} = (\sqrt{1/3}, \sqrt{1/3}, \sqrt{1/3})$, such that $r = 1$, we calculated in Fig. 2 the $\sigma_{|\Delta\vec{r}|}$ as a function of the angle $\varphi = \arccos(\vec{r}\cdot\vec{s})$ between the $\vec{s}$ and $\vec{r}$ vectors for two different $\sigma_s = 1.7\ 10^{-4}$ and $\sigma_s = 8.7\ 10^{-4}$ that correspond to a $\sigma_\theta = \sigma_\psi = 0.01°$ and $\sigma_\theta = \sigma_\psi = 0.05°$ angular resolution of the SSC system.

Equation (10) and Fig. 2 make it clear that the location resolution $\sigma_{|\Delta\vec{r}|}$ is drastically degraded when the SSC's axis becomes orthogonal to the vector $\vec{r}$. The dot product $(\vec{r}\cdot\vec{s})$ in the denominator of (10) comes close to zero in this case and all the $\sigma_{|\Delta\vec{r}|}$ components approach infinity. Inspecting (2), one can see that the $(\vec{r}\cdot\vec{s}) = 0$ simply degrades it. A single-point solution $r = (x, y, z)$ for a $(\vec{r}\cdot\vec{s}) \neq 0$ turns into a sphere $x^2 + y^2 + z^2 = r^2$ for any $(\vec{r}\cdot\vec{s}) = 0$.

One can see from Fig. 2 that an accurate ($\sigma_{|\Delta\vec{r}|} < 1$ mm) location tracking with a single three-axial transmitter is possible only if orientation freedom of the eye is limited, namely if $\varphi < 80°$ for a $\sigma_s = 1.7\ 10^{-4}$ and $\varphi < 60°$ for a $\sigma_s = 8.7\ 10^{-4}$.

It is important to note that employing an additional orthogonal search coil in the contact lens does not provide an escape from the above problem. It is so because the two orthogonal search coils can be oriented in such a way that their axes are perpendicular to the vector $\vec{r}$. The dot products $(\vec{r}\cdot\vec{s}_{\text{first coil}})$ and $(\vec{r}\cdot\vec{s}_{\text{second coil}})$ equal to zero in this case, and both systems of (2) describing the corresponding coil's location are degraded simultaneously.

III. EYE LOCATION TRACKING WITH A TRIAD OF THREE-AXIAL TRANSMITTERS

To track location of the SSCs with no orientation limitations, we suggest employing two more three-axial transmitters (three transmitters in all). The triad of transmitters can be located, for example, beneath the field coil box, as shown in Fig. 3. The distances r_1, r_2, and r_3 between the SSC and each of the transmitters in the triad can be found according to (3). Having a triad of distances, r_k, we can localize the SSCs by the triangulation technique.

To evaluate the location resolution, $\sigma_{|\Delta\vec{r}|}$, of the triangulation we should first examine the resolution σ_{r_k} of the distances r_k. Considering (11), we plotted in Fig. 4 the σ_{r_k} as a function of the angle $\varphi = \arccos(\vec{r}\cdot\vec{s})$ for an $r = 1$ m, $\sigma_{H_s} = 10^{-4}$, and two different $\sigma_s = 1.7\ 10^{-4}$ and $\sigma_s = 8.7\ 10^{-4}$.

Fig. 4 shows that the distance resolution σ_{r_k}—unlike the previously evaluated location resolution $\sigma_{|\Delta\vec{r}|}$ [see (10) and Fig. 2]—is practically not degraded no matter what is the SSC's orientation $\vec{s}$ relative to its location $\vec{r}$. Fig. 4 also shows tat the σ_{r_k} reaches its maximum value, $\sigma_{r_k\max}$, when the dot product $(\vec{r}\cdot\vec{s})$ becomes equal to zero ($\varphi = 90°$). This corresponds to the worst orientation of the SSC. It is important to note that the worst distance resolution, $\sigma_{r_k\max}$, is from two to four

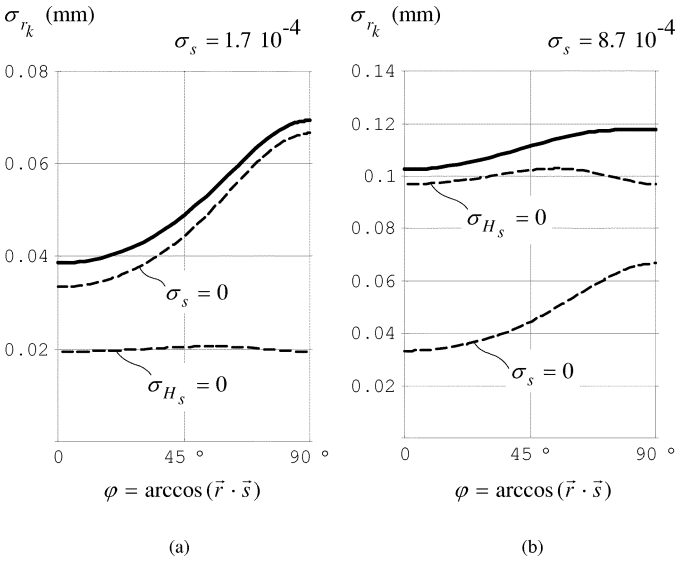

Fig. 4. The distance resolution σ_{r_j} as a function of the angle φ between the $\vec{r}$ and $\vec{s}$ vectors for an $r = 1$ m, $\sigma_{H_s} = 10^{-4}$, and two different $\sigma_s = 1.7\ 10^{-4}$ and $\sigma_s = 8.7\ 10^{-4}$ that correspond to a $\sigma_\theta = \sigma_\psi = 0.01°$ and $\sigma_\theta = \sigma_\psi = 0.05°$ angular resolution of the SSC system. The dashed lines show the σ_{r_j} components that are related to the different types of errors: the error in the coupling between the three-axial transmitter and the SSC, σ_{H_s}, and the error in the SSC's orientation, σ_s. One can see that the σ_{H_s} error dominates in (a) while the σ_s error dominates in (b).

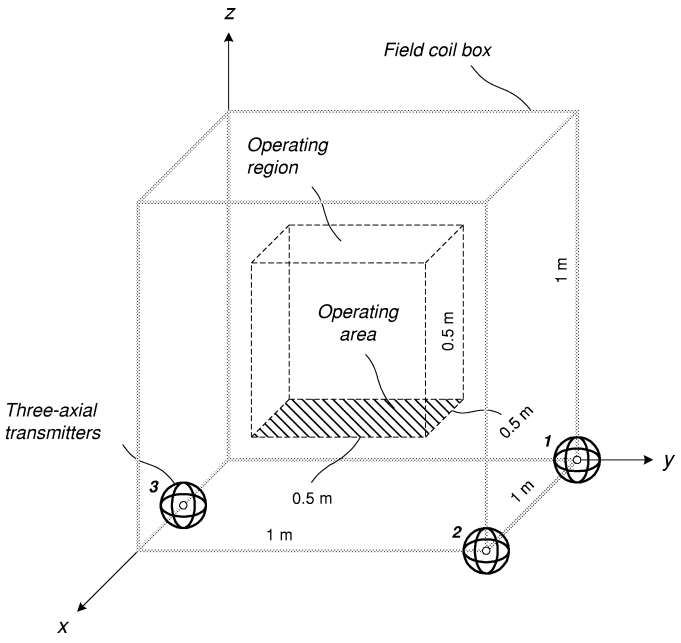

Fig. 5. Eye location tracking with a symmetrical triad of three-axial transmitters.

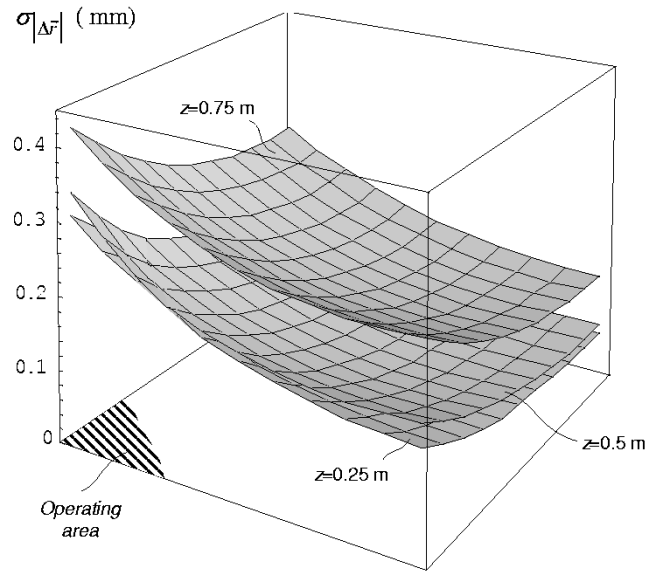

Fig. 6. The location resolution $\sigma_{|\Delta\vec{r}|}$ of the triangulation as a function of the SSC location (see Fig. 5) within the operating region ($\sigma_{H_s} = 10^{-4}$ and $\sigma_\sigma = \sigma_\psi = 0.01°$). In (a), the triad of transmitters is asymmetrical (see Fig. 4). In (b), the triad of transmitters is symmetrical (see Fig. 5). Note that in (b), the location resolution is below 0.3 mm over the whole operating region. This corresponds to a $3\sigma_{|\Delta\vec{r}|} \approx 1$ mm accuracy.

times better than the best (see Fig. 2) location resolution, $\sigma_{|\Delta\vec{r}|}$, reached with the single three-axial transmitter.

Now we can investigate the location resolution $\sigma_{|\Delta\vec{r}|}$ of the triangulation as a function of the SSC's location within the operating region in Fig. 5. We have done it considering for all the transmitters the average values of the distance rms error, $\sigma_{r_k\mathrm{av}}$. It should be a reasonable approximation because the SSC cannot be at the same time in its worst orientation relative to all the transmitters in the triad.

To calculate the $\sigma_{|\Delta\vec{r}|}$, we substituted all possible combinations of the $r_{k\min} = r_k - \sigma_{r_k\mathrm{av}}$ and $r_{k\max} = r_k + \sigma_{r_k\mathrm{av}}$ in the following triangulation equations:

$$\begin{cases} \hat{x} = 0.5(1 + r_1^2 - r_2^2) \\ \hat{y} = 0.5(1 - r_1^2 + r_3^2) \\ \hat{z} = 0.5\sqrt{2(r_2^2 + r_3^2 - 1) + 2r_1^2(r_2^2 + r_3^2) - 2r_1^4 - r_2^4 - r_3^4} \end{cases} \quad (12)$$

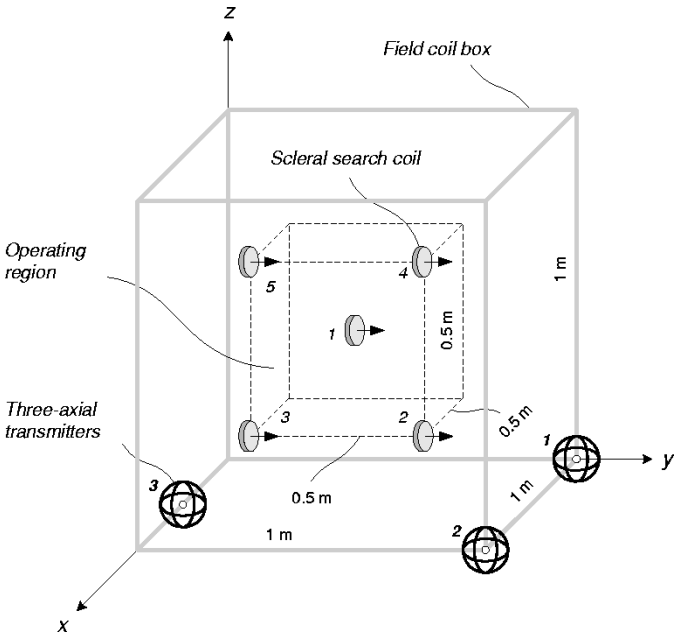

Fig. 7. The location tracker configuration used for the simulation of the method (see Fig. 8).

where $(\hat{x}, \hat{y}, \hat{z})$ are estimates of the SSC's coordinates. After finding all the possible $(\hat{x}, \hat{y}, \hat{z})$ combinations, we calculated

$$\sigma_{|\Delta\vec{r}|} = \mathrm{Max}\left[\sqrt{(\hat{x}-x)^2 + (\hat{y}-y)^2 + (\hat{z}-z)^2}\right] \quad (13)$$

where (x, y, z) are the true SSC's coordinates.

Fig. 6(a) shows the results of the above calculations obtained for a $\sigma_{H_s} = 10^{-4}$ and $\sigma_s = 1.7\,10^{-4}$ ($\sigma_\sigma = \sigma_\psi = 0.01°$). One can see from this figure that asymmetric location of the three-axial transmitters in Fig. 3 causes an asymmetric, nonoptimal distribution of the rms error $\sigma_{|\Delta\vec{r}|}$ over the operating area.

The above distribution of the $\sigma_{|\Delta\vec{r}|}$ can be improved [see Fig. 6(b)] for a symmetric triad of transmitters shown in Fig. 5.

One can see from Fig. 6(b) that the location resolution is better than 0.3 mm throughout the operating region. This corresponds to an $3\sigma_{|\Delta\vec{r}|} \approx 1$ mm accuracy of the method.

IV. Simulation of the Method

Our final aim is to confirm with the help of computer simulations the analytical results obtained in the previous section. We have done it for the SSC system whose configuration is shown in Fig. 7.

Parameters of the three-axial transmitters and the SSC were chosen in accordance with Table I. The SSC was situated in various locations throughout the operating region as shown in Fig. 8. For the each location, we calculated the true components of the $\vec{H}_s$ vector according to (2). Then we added samples of uncorrelated white noise signals ξ_{s_j} with a $\sigma_s = 1.7\,10^{-4}$ and $\xi_{H_{si}}$ with a $\sigma_{H_s} = 10^{-4}$ to the corresponding true components of the $\vec{s}$ and $\vec{H}_s$ vectors. Substituting the noisy components of the above vectors into (3), we obtained the noisy distances, r_k, between the SSC and the transmitters. Then, we calculated the SSC's coordinates by substituting the noisy r_k into the triangulation equations written for the chosen triad configuration (see Fig. 7). The above procedure was repeated 500 times for the each location of the SSCs in Fig. 7.

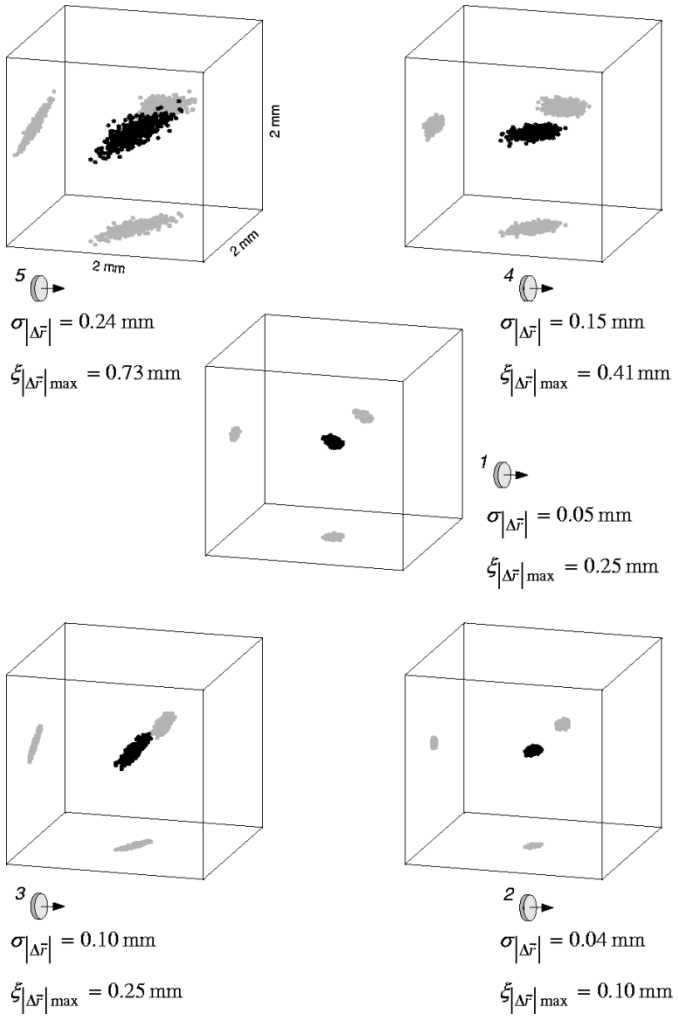

Fig. 8. Simulation of the SSC's location estimates for a $\sigma_{H_s} = 10^{-4}$, $\sigma_\theta = \sigma_\psi = 0.01°$. The SSC is situated in various locations throughout the operating region (see Fig. 7). Each cube corresponds to a $2 \times 2 \times 2$ mm space around the true SSC's location. The black dots within the cubes represent the location estimates (500 total for each cube). The gray dots on the cubes' facets are projections (shadows) of the dots within the cube.

Eventually, the location estimates were plotted in Fig. 8 within a $2 \times 2 \times 2$ mm cubic space around the true SSC's location. Both the rms $\sigma_{|\Delta\vec{r}|}$ and maximum $\xi_{|\Delta\vec{r}|_{\max}}$ errors were calculated and are given in Fig. 8.

A comparison between Figs. 8 and 6(b) shows a good agreement between the simulations and the theoretical calculations.

V. Conclusion

Section II demonstrates that supplying a typical SSC system with a single three-axial transmitter allows a *direct* location tracking of the eye. Analytical equations describing the eye coordinates, $\vec{r} = (x, y, z)$, and the distance, r, between the eye and the three-axial transmitter involve the eye orientation components, $\vec{s} = (s_1, s_2, s_3)$, (measured by the SSC system) along with the components, $\vec{H}_s = (H_{s1}, H_{s2}, H_{s3})$, of the magnetic coupling between the three-axial transmitter and the SSC. The error analysis of the equations developed shows that the location resolution, $\sigma_{|\Delta\vec{r}|}$, is drastically degraded when the SSC's axis,

$\vec{s}$, becomes orthogonal to the vector $\vec{r}$. It means that an accurate location tracking with a single three-axial transmitter is possible only if orientation freedom of the eye is limited.

In Section III, we discover and take advantage of the important fact that the resolution of the distance, r, between the eye and the three-axial transmitter is hardly affected by the relative orientation of the $\vec{s}$ and $\vec{r}$ vectors. Moreover, the average distance resolution, $\sigma_{r_k} = \sigma_{r_{k\mathrm{av}}}$, (see. Fig. 4) is found to be from two (for $\sigma_s = 1.7\ 10^{-4}$) to four (for $\sigma_s = 8.7\ 10^{-4}$) times better than the best location resolution, $\sigma_{|\Delta\vec{r}|}$ (see. Fig. 2). Considering the above facts, we suggest supplying a typical SSC system with a triad of three-axial transmitters and employ the triangulation technique to track the eye location with no orientation limitations.

In Section IV, the location resolution of the triangulation is analyzed both analytically and numerically, and a good agreement between the analytical and numerical results is found. It is shown that the location tracking accuracy can be as good as ± 1 mm (in a 200-Hz bandwidth) throughout a relatively large ($0.5 \times 0.5 \times 0.5$ m) operating region in the center of a $1 \times 1 \times 1$ m SSC system.

It should be noted that in practical implementations of the proposed method, both the location resolution and the eye orientation resolution can be reduced due to the inevitable crosstalk between the location-tracking transmitters and the SSC system itself. The importance of the present paper is in finding the theoretical limits for the eye location resolution.

ACKNOWLEDGMENT

The authors wish to thank Dr. J. Tabrikian for his helpful suggestions and comments.

REFERENCES

[1] D. A. Robinson, "A method of measuring eye movements using a scleral search coil in a magnetic field," *IEEE Trans. Biomed. Eng.*, vol. BME-10, pp. 137–145, 1963.

[2] R. S. Remmel, "An inexpensive eye movement monitor," *IEEE Trans. Biomed. Eng.*, vol. BME-31, pp. 388–390, 1984.

[3] H. J. Kasper and B. J. Hess, "Magnetic search coil system for linear detection of three-dimensional angular movements," *IEEE Trans. Biomed. Eng.*, vol. 38, pp. 466–475, May 1991.

[4] Search Coil Eye Movement Monitors [Online]. Available: http://graybiel.cc.brandeis.edu/coil.htm

[5] [Online]. Available: http://www.ascension-tech.com/

[6] A. Matveyev, *Principles of Electrodynamics*. New York: Reinhold, 1966.

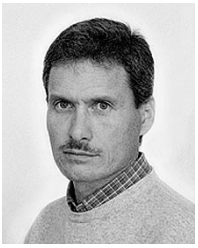

Eugene Paperno received the B.Sc. and M.Sc. degrees in electrical engineering from the Minsk Institute of Radio Engineering, Minsk, Republic of Belarus, in 1983. In 1997, he received the Ph.D. degree (*summa cum laude*) from the Ben-Gurion University of the Negev, Beer-Sheva, Israel.

From 1983–1991, he was with the Institute of Electronics, Belorussian Academy of Sciences. From 1992-1997, he was a Teaching Assistant with the Department of Electrical and Computer Engineering of the Ben-Gurion University of the Negev. From 1997–1999, he was a JSPS Postdoctoral Fellow with Kyushu University, Fukuoka-shi, Japan. Since 1999, he is with the Department of Electrical and Computer Engineering, Ben-Gurion University of the Negev. His current interests include magnetic tracking systems for human computer interface and virtual reality systems.

Dmitry Semyonov received the B.Sc. degree in biomedical engineering from the Taganrog Radio-Technical University, Taganrog, Russia in 1997. Since 2001, he is working towards the M.Sc. degree at the Department of Biomedical Engineering of the Ben-Gurion University of the Negev, Beer-Sheva, Israel.

He is a Teaching Assistant with the Department of Biomedical Engineering of the Ben-Gurion University of the Negev. His current interests are magnetic tracking systems for monitoring eye movements in man and experimental animals.